Received: 15 August 2023 | Revised: 30 January 2024 | Accepted: 13 April 2024

DOI: 10.1002/ecy.4404

ARTICLE

ECOLOGY
ECOLOGICAL SOCIETY OF AMERICA

It's about (taking up) space: Discreteness of individuals and the strength of spatial coexistence mechanisms

Stephen P. Ellner[1] | **Robin E. Snyder**[2] | **Peter B. Adler**[3] | **Christina M. Hernández**[1,4] | **Giles Hooker**[5,6]

[1]Department of Ecology and Evolutionary Biology, Cornell University, Ithaca, New York, USA

[2]Department of Biology, Case Western Reserve University, Cleveland, Ohio, USA

[3]Department of Wildland Resources & The Ecology Center, Utah State University, Logan, Utah, USA

[4]Department of Biology, Oxford University, Oxford, UK

[5]Department of Statistics and Data Science, Cornell University, Ithaca, New York, USA

[6]Department of Statistics and Data Science, University of Pennsylvania, Philadelphia, Pennsylvania, USA

Correspondence
Stephen P. Ellner
Email: spe2@cornell.edu

Funding information
NSF, Grant/Award Numbers: DEB-1933497, DEB-1933561, DEB-1933612

Handling Editor: Caz M. Taylor

Abstract

One strand of modern coexistence theory (MCT) partitions invader growth rates (IGR) to quantify how different mechanisms contribute to species coexistence, highlighting fluctuation-dependent mechanisms. A general conclusion from the classical analytic MCT theory is that coexistence mechanisms relying on temporal variation (such as the temporal storage effect) are generally less effective at promoting coexistence than mechanisms relying on spatial or spatiotemporal variation (primarily growth-density covariance). However, the analytic theory assumes continuous population density, and IGRs are calculated for infinitesimally rare invaders that have infinite time to find their preferred habitat and regrow, without ever experiencing intraspecific competition. Here we ask if the disparity between spatial and temporal mechanisms persists when individuals are, instead, discrete and occupy finite amounts of space. We present a simulation-based approach to quantifying IGRs in this situation, building on our previous approach for spatially non-varying habitats. As expected, we found that spatial mechanisms are weakened; unexpectedly, the contribution to IGR from growth-density covariance could even become negative, opposing coexistence. We also found shifts in which demographic parameters had the largest effect on the strength of spatial coexistence mechanisms. Our substantive conclusions are statements about one model, across parameter ranges that we subjectively considered realistic. Using the methods developed here, effects of individual discreteness should be explored theoretically across a broader range of conditions, and in models parameterized from empirical data on real communities.

KEYWORDS
coexistence, coexistence mechanisms, growth-density covariance, individual-based model, lottery model, partitioning, spatial heterogeneity, storage effect

INTRODUCTION

The mathematical theory underpinning "Modern Coexistence Theory" (MCT; Chesson, 1994; Chesson & Warner, 1981) was developed to support the hypothesis that temporal variability in environmental conditions might contribute to species coexistence (Grubb, 1977; Hutchinson, 1961) rather than just hastening the chance extinction of species

(May & MacArthur, 1972), and to identify the conditions required for that to happen. These analyses were later extended to coexistence mechanisms resulting from spatial variability, either on its own or in combination with temporal variability (Chesson, 1985, 2000a; Johnson & Hastings, 2023; Snyder, 2008; Snyder & Chesson, 2003, 2004).

One general conclusion from models with both spatial and temporal variation is that temporal variation is generally less effective at promoting coexistence than comparably large spatial or spatiotemporal variation, except in the limit of extremely long organism lifetimes, so long as the spatial scale of organismal dispersal or undirected movement is small enough that each species can become concentrated in areas where it performs best. "Coexistence is most likely to occur when all variation is some combination of spatiotemporal and spatial variation: pure temporal variation promotes coexistence less effectively than these other two forms of variation" (Chesson, 1985, p. 269). "Mechanisms relying on spatial variation have already been shown to be far stronger than the temporal storage effect (Snyder, 2008)" (Stump & Vasseur, 2023).

However, those conclusions were obtained in the framework of classical analytic MCT, which makes potentially important assumptions. Specifically, the landscape is assumed to be infinitely large relative to the size of an individual, population densities are treated as continuous, and coexistence is analyzed by asking whether an extremely rare species (the "invader") will have a positive long-term population growth rate. Technically, "extremely rare" means that population growth rate is calculated by linearizing the invader's population dynamics at zero population density, and "long-term" means a theoretical average over infinite time. An invader is thus given infinite amounts of time to spread across the entire available landscape, and to find and cluster in the most advantageous locations. Moreover, after both those occur, the invader is assumed to still be so rare that it experiences no intraspecific competition at all while recovering from the brink of extinction.

Giving a rare species unlimited opportunity to cluster in the best locations, and then unlimited time to expand without ever experiencing intraspecific competition, are surely the ideal assumptions for maximizing the impact of spatial variability on coexistence. Are those unrealistic features possibly the real reason why spatial variation has been found to have such a "large potential to promote coexistence" (Snyder, 2008, p. 130), relative to temporal variation?

These unrealistic features of the classical theory are easy to deride, but at the same time, it is not clear if they constitute an actual problem or a manageable complication. Differential and difference equation models allow fractional individuals, and thus allow populations to rebound from minuscule densities (in the absence of strong Allee effects). But we do not abandon them because of that flaw. Instead, we try to "throw out the bathwater" but "keep the baby"—we identify and disregard behaviors that only occur because we have ignored the true discreteness of individuals and the finite extent of the landscape, and learn from conclusions that are not artifacts of that unrealistic assumption.

Previous work has shown that spatial clustering makes it harder to escape intraspecific competition. For example, Murrell (2010) studied how individual discreteness and clustering due to limited dispersal affected fluctuation-independent coexistence in a spatial, individual-based Lotka–Volterra model. Although the landscape was assumed to be homogenous, limited-range dispersal caused clustering and increased the intensity of intraspecific competition. As a result, the species with stronger intraspecific competition could be excluded from the community for parameters where coexistence would occur in the Lotka–Volterra differential equations, or in the same spatial model with long-range interactions. This outcome reverses the classical prediction from Lotka–Volterra type models that stronger intraspecific competition promotes coexistence of competitors (e.g., Chesson, 2000b, p. 345). However, Murrell (2010, p. 1615) speculated that interspecific differences in "habitat requirements, for example, for soil depth or slope/elevation, will overcome the negative impact of within-species clustering."

In the predecessor to this paper (Ellner et al., 2022, hereafter, DS22), we explored how the spatial distribution of discrete individuals affected coexistence based on purely temporal fluctuations: storage effect, and relative nonlinearity of competition. Analogous to Murrell (2010), we found that the natural clustering of a rare species hindered coexistence. Even when rare, each species experiences elevated competition when conditions are favorable for reproduction, creating positive environment-competition covariance and thus weakening the storage effect.

Here, we extend our model and analysis to include spatial variability and spatial coexistence mechanisms, to begin sorting "baby" from "bathwater" with regard to the relative strength of coexistence mechanisms based on spatial variability when individual discreteness is acknowledged. We anticipated that individual discreteness would weaken spatial coexistence mechanisms. The classical theory (Snyder, 2008) says that the dominant spatial mechanism is growth-density covariance arising from a rare invader clustering in its preferred part of the

habitat, while the resident is most abundant elsewhere. With discrete individuals, that benefit would be reduced by intraspecific competition even when an invader is rare. Classically, the key parameter for the strength of spatial mechanisms is the dispersal range of the invading species, because it determines whether the lineage initiated by a well-situated invader remains in good habitat. We expected that to remain true.

We tested these hypotheses through a simulation study that factorially varied the competing species' dispersal ranges, the spatial scale of habitat heterogeneity, the strength of intraspecific competition, and the magnitudes of spatial and temporal variability. In the process, we illustrate general methods that can be used to extend this study to other models, and to ask other questions about spatial coexistence mechanisms where discreteness of individuals may be important.

Our approach has much in common with the Johnson and Hastings (2023) analysis of coexistence mechanisms in spatiotemporally fluctuating environments. Like Chesson (2000a) and Johnson, Hastings (2023) assumed continuous population densities for a population distributed in discrete habitat patches, so our methods differ from theirs, but many conceptual aspects are the same.

THE MODEL

Our notation is summarized in Table 1. As in DS22, the model is a spatially explicit version of the classical lottery model of competition for space in a temporally varying environment (Chesson & Warner, 1981). The classical lottery model considers a habitat consisting of N sites, with one adult occupying each site. Within year t, first each species-q adult produces $\beta_q(t)$ larvae in year t, which are then dispersed evenly to all sites. Following this, some adults die (with per capita mortality rate δ_q) and a new occupant is chosen for each vacated site by a fair "lottery": unbiased random choice of one individual from all larvae at the site.

The original lottery model is a mean-field model for expected population change each year, given the fecundities $\beta_q(t)$. When there are two species occupying $N_1(t)$ and $N_2(t)$ sites respectively, $N_1(t)+N_2(t)\equiv N$ and the model can be written as

$$N_1(t+1)=\underbrace{N_1(t)(1-\delta_1)}_{\text{Survivors}}+\underbrace{[\delta_1 N_1(t)+\delta_2(N-N_1(t))]}_{\text{Number of open sites}}\times\underbrace{\frac{\beta_1(t)N_1(t)}{\beta_1(t)N_1(t)+\beta_2(t)(N-N_1(t))}}_{\text{Chance to win an open site}}. \quad (1)$$

This model is spatially implicit: site locations are immaterial because larvae disperse uniformly across all sites.

DS22 made two qualitative changes to the classical lottery model, both retained here. First, the model was implemented as a finite-population individual-based model, tracking discrete adults occupying M^2 sites in a finite square lattice. Second, the model was made spatially explicit, with dispersal kernels specifying how larvae produced at any one site $x=(x_1,x_2)$ are scattered among sites in the lattice, and a competition neighborhood such that adult fecundity is reduced by the presence of conspecifics (rather than allospecifics) within their neighborhood.

Specifically, larval dispersal from site x to site x' depends on distance (d) between the sites defined as

$$d(x',x)=\mathbf{max}\left(\left|x_1'-x_1\right|,\ \left|x_2'-x_2\right|\right). \quad (2)$$

The dispersal kernel is defined so that the fraction of larvae dispersed to sites x' at distance d is proportional to $e^{-\alpha d}$, $\alpha\geq 0$ (ignoring edge effects). Larvae that would disperse off the lattice based on distance are re-distributed to sites in the lattice, in proportion to the kernel values at those sites. That is, kernels that extend past the edge of the lattice are re-scaled so as not to lose larvae. Numerical experiments showed that our simulated lattice is large enough that the assumed fate of larvae from parents near the lattice edge is unimportant; see Appendix S1: Section S1. We also imposed a maximum dispersal distance of 15, to avoid artifacts of "nano-larvae" dispersing very large distances, while still allowing each species to disperse some larvae into clusters of the other species when α is small. Larval dispersal is described by a mean-field equation for the expected number of larvae landing at each site, given the location and fecundity of all adults, while adult mortality and the lottery for vacated sites are both done as individual-by-individual "coin tossing" simulations. Deterministic larval dispersal reduces our parameter space, because it implies that only relative fecundities matter, not absolute fecundities. In DS22 we found that demographic stochasticity in adult mortality had only trivial effects (the same is true here), so on the assumption that larvae vastly outnumber adults, it is safe to ignore demographic stochasticity in larval dispersal.

The adult competition neighborhood for the individual at x consists of all sites at distances d between 1 and some integer k, where distance is calculated as for dispersal. DS22 considered $k=1$, 2, and 3, but the strengths of coexistence mechanisms showed the same qualitative trends in response to changes in model parameters for all values of k, so here we just use $k=2$. The effect of

TABLE 1 Notation and definitions.

Notation	Formula and/or meaning
Varied parameters	
α	Dispersal distance scaling parameter, same for both species. Dispersal is proportional to $e^{-\alpha d}$, $\alpha \geq 0$.
a_q	Intraspecific competition strength parameter for species q adults. Competition reduces per-capita fecundity from its maximum, $\beta_q(x,t)$, by the factor $1/\left(1+a_q f_q\right)$.
D	Distance scale of permanent spatial variation in $\mathbf{P}_q$.
$\sigma_{P,q}$	Spatial environmental SD. Multiplies $P_{q,i,j}$ in computing $\beta_q(x,t)$.
$\sigma_{W,q}$	Temporal environmental SD. Multiplies $W_q(t)$ in computing $\beta_q(x,t)$.
δ_q	Per-capita adult mortality rate of species q.
ρ_W	Between-species correlation of random temporal variation W at any one time t.
ρ_P	Between-species correlation of permanent spatial variation $\mathbf{P}$ at any one lattice site.
Other parameters and variables	
$N_q(t)$	Total population of species q at time t, in terms of the no. sites occupied by an adult.
$n_q(x,t)$	The population of species q at site x and time t, either 0 or 1.
$\beta_q(x,t)$	Maximum per-capita fecundity of species q at location x, time t.
μ_q	The overall expectation of per-capita fecundity $\mathbb{E}\left[\log\beta_q\right]$.
f_q	Fraction of sites occupied by species q in an individual's competition neighborhood.
$\mathbf{P}_q$	Permanent spatial variation affecting species q. This matrix has entries $P_{q,i,j}$. We specify that its spatial mean is 0, and its spatial variance is 1.
$W_q(t)$	Random temporal variation affecting species q at all locations, time t.
r_q	Long-run growth rate of species q, also referred to as $\log\ \lambda_{S,q}$.
$\lambda_q(x,t)$	Local population growth rate, defined as $\overline{R}_q(x,t)+\left(1-\delta_q\right)$.
$\nu_q(x,t)$	Local population density of species q, defined as $n_q(x,t)/\langle n_q(t)\rangle$.
$\overline{R}_q(t)$	Expected no. species q recruits at time t.
$\eta_q(t)$	Demographic stochasticity for species q at time t.
$E_q(x,t)$	Environment experienced by species q at location x, time t. Equal to $\beta_q(x,t)$.
$C_q(x,t)$	Competition experienced by species q at location x, time t. Equal to $\beta_q(x,t)/\overline{R}_q(t)$.
$E_q^{\#}(x,t)$	Environment experienced by species q, generated independently from $C_q(x,t)$.
χ_q	The population growth measure being partitioned, here the IGR $\mathbb{E}\left[r_q\right]$.
$\varepsilon_{q,k}$	fANOVA contribution of feature k for species q.
Δ_k	Invader-resident comparison $\varepsilon_{ik}-\varepsilon_{rk}$.
$\bullet^{(j,v,k)}$	Quantity $\bullet$ for replicate j with vacancy configuration v and lattice configuration k, for example, $C_q^{(j,v,k)}(t)$ in one-step-ahead simulations.
J	No. replicates per vacancy configuration in one-step-ahead model simulations.
K	No. lattice configurations used in one-step-ahead model simulations.
V	No. vacancy configurations per lattice configuration in one-step-ahead model simulations.

Note: The model parameters that are varied in simulations are in the upper block of the table.

competition is that the maximum per-capita fecundity $\beta_q(t)$ for a species q individual is reduced by a fraction $1/\left(1+a_q f_q\right)$ where f_q is the fraction of species-q individuals in the individual's competition neighborhood. The parameter a_q thus measures the strength of intraspecific competition relative to interspecific competition.

In this paper, we extend the DS22 model by assuming that the maximum per-capita fecundities β_q vary across space, not just over time. That is, instead of one $\beta_q(t)$

value for all species q adults in year t, we have $\beta_q(x,t)$ for each site x in the lattice. Specifically, we assume that $\log\beta$ is the sum of three components: an overall expectation, permanent spatial variation in intrinsic site quality for each species, and random temporal variation that is the same at all spatial locations for each species.

1. The overall expectation $\mathbb{E}[\log\beta_q]$ is denoted μ_q.
2. The *permanent spatial variation* for species q is represented by a matrix $\mathbf{P}_q$ with entries $P_{q,i,j}$. Without loss of generality, we assume that the spatial average of $\mathbf{P}_q$ is zero, and that its spatial variance equals 1. $\mathbf{P}_q$ is characterized by its spatial correlation scale D (see Figure 1) which determines the typical size of "good habitat" patches for each species, and by the between-species correlation at each site $\rho_{B,P} < 0$, representing specialization on different types of habitat.
3. The *random temporal variation* for species q is represented by the scalar stochastic process $W_q(t)$ (the "weather"). W_q has mean 0 and variance 1, and is characterized by its cross-species correlation $\rho_{B,W}$. We assume for simplicity that each $W_q(t)$ series is temporally uncorrelated, but we assume a negative cross-species correlation to represent specialization on different "temporal niches."

We then specify that at location $x=(i,j)$ the maximum per-capita fecundity β_q for a species q individual is defined by

$$\log\beta_q(x,t) = \mu_q + \sigma_{P,q}P_{q,i,j} + \sigma_{W,q}W_q(t), \qquad (3)$$

where σ_P and σ_W are the SDs of the permanent spatial variation and the random temporal variation, respectively. The realized per-capita fecundity, resulting from the effect of neighborhood competition, is $\beta_q(x,t)/\left(1+a_q f_q(x,t)\right)$ where $f_q(x,t)$ is the fraction of species-q individuals in the competition neighborhood centered at site x in year t.

The interpretation of the variance parameters σ is complicated by the log on the left-hand side. Because of this, larger values of μ will produce higher variance in β for the same values of σ_P and σ_W. To mitigate this property, we set $\mu_1 = 0$. This entails no loss of generality because only the ratios $\beta_1(x,t)/\beta_2(x,t)$ matter for the dynamics. We can therefore divide all $\beta_q(x,t)$ by $\exp(\mu_1)$ without changing anything, and that is equivalent to setting $\mu_1 = 0$. (We will later set $\mu_2 < 0$ to create a small mean fitness disadvantage for the invader.) W and each entry in $\mathbf{P}$ were assumed to have truncated Normal distributions. For additional details on how $\mathbf{P}$ matrices were generated, see Appendix S1: Section S2.

METHODS: THEORY

Invader growth rate

Following Ellner et al. (2019) and DS22, we study coexistence by using model simulations to compute invader growth rate (IGR) $\mathbb{E}[r_q]$ for a species q that has become rare. With discrete individuals, we cannot use the classical definition of IGR based on a limit as invader abundance falls to 0. IGR then unavoidably depends on how "rare" is defined. As we discuss in DS22 (section S2 of the Supplement to that paper), simulation studies suggest that the best available definition is the expected growth rate during one time step, when a species has become just common enough for the risk of extinction in one or two time steps to be small. Whether the rare population then tends to grow or shrink from one year to the next determines if it is likely to increase and persist, or instead shrink and soon perish due to chance mortality of all survivors at once. The MCT approach of characterizing coexistence through behavior near extinction boundaries, when a disturbance or string of bad luck has reduced a species to very low abundance, is conceptually very similar to the ideas of permanence (Hutson & Schmitt, 1992) and uniform persistence (Smith & Thieme, 2011) for deterministic dynamical systems: however close it comes to extinction, for whatever unusual reason, can each species rebound and rejoin the community?

Using IGR to characterize coexistence has become somewhat controversial because the relationship between IGR and mean persistence time can be non-monotonic in theory (Pande et al., 2020). One strong justification for studying IGR is that the sign of IGR distinguishes two distinct scaling regimes for mean persistence time as a function of total community size, so that a positive value is required for long-term persistence (see Ellner et al., 2020, and DS22 [p. 21 and Appendix S1: Section S1]). To our knowledge, qualitative disagreement between IGR and other persistence metrics has not yet been demonstrated in any empirically parameterized model (e.g., in fig. 4b of Pande et al. (2020), qualitative disagreement only arises if mean adult longevity is deliberately reduced by a factor of 10 or more).

To compare the strength of spatial and temporal variability mechanisms, we also partition $\mathbb{E}[r_q]$ into contributions from different coexistence mechanisms and their interactions. We focus on the canonical partition of IGR into contributions from storage effect, relative nonlinearity in competition, relative nonlinearity in environment, growth-density covariance, and fluctuation-independent mechanisms (such as resource partitioning) (Chesson, 1994, 2000a).

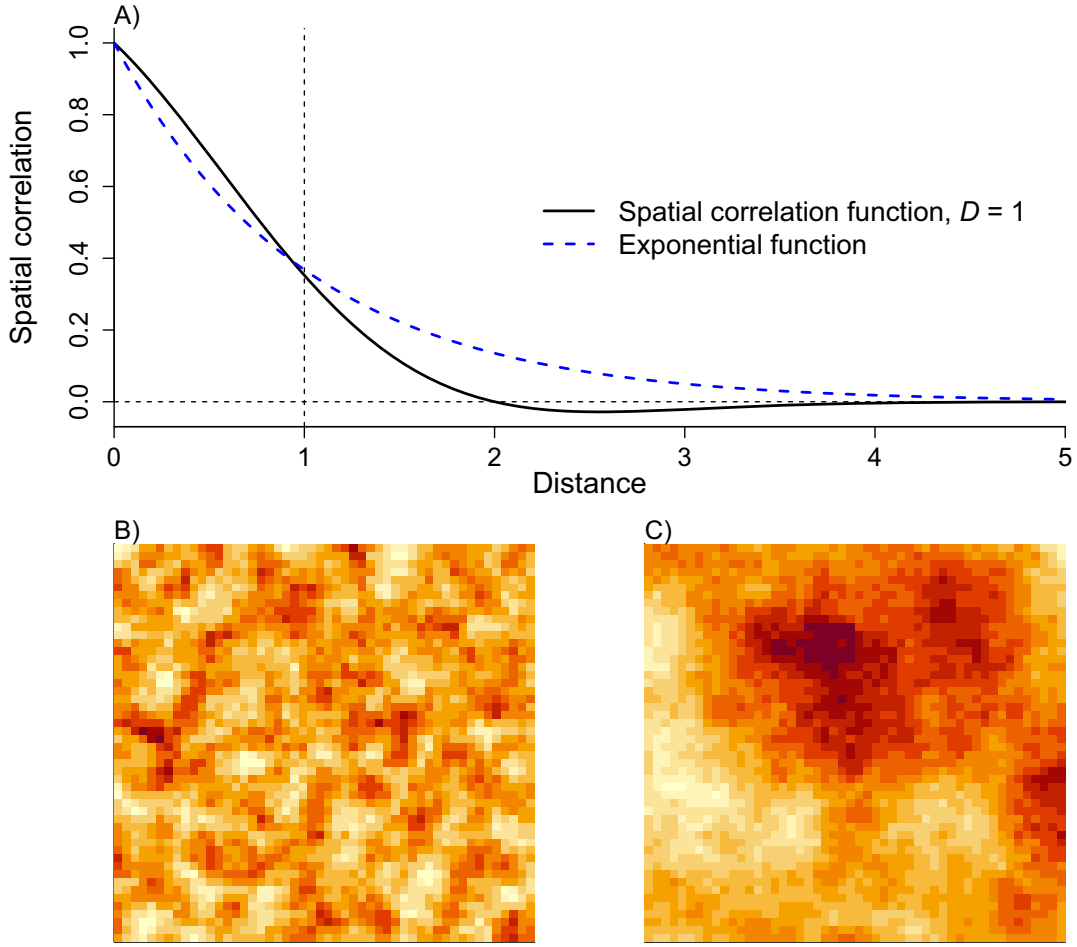

FIGURE 1 (A). The spatial correlation function used in this paper (black solid line) compared with an exponentially decaying correlation function (blue dashed line). The spatial correlation at distance d, when the correlation scale is D, is given by $\rho_S(d) = (1 - z/2)e^{-0.35z^2}$ where $z = d/D$. For distances 0 to D this is nearly equal to exponential decrease of correlation with distance ($\rho = e^{-d/D}$). At greater distances it falls off faster, becoming weakly negative at $d = 2D$, resulting in more clearly defined patches of good and bad habitat than result from exponential decay. (B). An example of a simulated 50×50 lattice $\mathbf{P}$ with $D = 2$; darker color indicates better habitat quality for one of the species. (C) A simulated lattice with $D = 12$. Figure made by R script `MakeCorrelatedLattices.R` available at https://doi.org/10.6084/m9.figshare.23926179.

Let $\overline{\cdot}$ denote an expectation and let $\langle \cdot \rangle$ denote a spatial average. Let $n_q(x,t)$ be the number of species q adults at site x at time t, which is either 0 or 1. The *local* population growth rate $\lambda_q(x,t)$ is defined as the expected number of recruits (i.e., number of vacated sites won) that would be produced by a species q adult at location x at time t (denoted $\overline{R}_q(x,t)$), plus the probability of the parent surviving:

$$\lambda_q(x,t) = \overline{R}_q(x,t) + (1 - \delta_q). \tag{4}$$

Note, there may or may not be a species q parent at x at time t; $\lambda_q(x,t)$ is nonetheless well defined as what *would* hold if site x is occupied by species q. The formula for $\overline{R}_q$ is derived in Appendix S1: Section S4.

Because $n_q(x,t) = 0$ or 1, the expected spatially averaged population at the next time step is given by

$$\mathbb{E}\langle n_q(t+1)\rangle = \langle \lambda_q(x,t) n_q(x,t)\rangle. \tag{5}$$

The spatially averaged actual population is

$$\langle n_q(t+1)\rangle = \langle \lambda_q(x,t) n_q(x,t)\rangle \eta_q(t), \tag{6}$$

where Equation (6) defines $\eta_q(t)$, our measure of demographic stochasticity. That is, $\eta_q(t)$ is the factor by which the actual total population for species q differs from the expected total population.

Following Chesson's approach, we define the overall population growth rate $\tilde{\lambda}_q(t)$ by writing

$$\begin{aligned}\langle n_q(t+1)\rangle &= \left(\langle\lambda_q(t)\rangle\langle n_q(t)\rangle + Cov\left(\lambda_q(t), n_q(t)\right)\right)\eta_q(t)\\ &= \underbrace{\left(\langle\lambda_q(t)\rangle + \mathrm{Cov}\left(\lambda_q(t), \nu_q(x,t)\right)\right)}_{\tilde{\lambda}_q(t)}\eta_q(t)\langle n_q(t)\rangle,\end{aligned} \tag{7}$$

where $\nu_q(x,t) = n_q(x,t)/\langle n_q(t)\rangle$. Because population growth is multiplicative, IGR is given by the log of the stochastic growth rate λ_S, where $\log\lambda_S$ is defined as the average over many time steps of

$$\log\frac{\langle n_q(t+1)\rangle}{\langle n_q(t)\rangle} = \log\left(\tilde{\lambda}_q(t)\eta_q(t)\right). \tag{8}$$

Thus, the IGR to be partitioned is

$$\begin{aligned}\mathbb{E}\left[r_q\right] &= \mathbb{E}\left[\log\lambda_{S,q}\right] = \mathbb{E}\left[\log\left(\tilde{\lambda}_q(t)\eta_q(t)\right)\right]\\ &= \mathbb{E}\left[\log\tilde{\lambda}_q(t)\right] + \mathbb{E}\left[\log\eta_q(t)\right],\end{aligned} \tag{9}$$

where the right-hand side is evaluated for population states in which the focal species q is rare, but not so rare that its dynamics are dominated by demographic stochasticity (see DS22, Appendix S1: Section S2).

Partitioning IGR into coexistence mechanisms

The canonical MCT coexistence mechanisms are based on expressing population growth as a function of environmental (E) and competition (C) factors, where E represents the potential for population growth for a given set of abiotic conditions and C is the reduction of population growth due to competition. For lottery models this is generally done by defining

$$\begin{aligned}E_q(x,t) &= \beta_q(x,t),\\ C_q(x,t) &= \beta_q(x,t)/\overline{R}_q(x,t).\end{aligned} \tag{10}$$

Thus E is the maximum per-capita fecundity under current conditions, while E/C is the expected actual number of recruits produced per adult ("expected" because these definitions involve the expected net outcome from the lotteries at each vacant site, not the actual outcomes in a given year). With these definitions,

$$\lambda_q(x,t) = \left(1-\delta_q\right) + E_q(x,t)/C_q(x,t). \tag{11}$$

For $\beta_q = 0$ we let C_q equal the limiting value of the above definitions as $\beta_q \to 0$; see Appendix S1: Section S4 for details.

As in DS22 (and much like Johnson and Hastings [2023]), we partition the IGR (Equation 9) using a simulation-based functional analysis of variance (fANOVA) approach (Ellner et al., 2019) rather than the small-variance approximations of analytic MCT (Chesson, 1994, 2000a; Johnson & Hastings, 2023; Snyder, 2008; Snyder & Chesson, 2003, 2004). With E and C defined so that the local growth rates λ_q are a function of E and C, the IGR can be written as

$$\begin{aligned}\mathbb{E}\left[r_q\right] = \mathbb{E}\ \log\Bigg[&\underbrace{\left\langle\lambda_q\left(E_q(x,t), C_q(x,t)\right)\right\rangle}_{\overline{\lambda}(t)}\\ &+ Cov_x\left(\lambda_q(x,t)\nu_q(x,t)\right)\Bigg] + \mathbb{E}\ \log\eta(t).\end{aligned} \tag{12}$$

fANOVA is the general name for several ways of decomposing a nonlinear function of many variables into a sum of main effects of each variable, and their 2-way, 3-way, and so forth. interactions. Given a function $\chi(x_1, x_2, ..., x_d)$ that can be evaluated numerically, an fANOVA decomposition has the general form

$$\begin{aligned}\chi(x_1, x_2, \cdots, x_d) = &\underbrace{\varepsilon^0}_{\text{Baseline}} + \underbrace{\sum_i \varepsilon^i(x_i)}_{\text{Main effects}} + \underbrace{\sum_{i\neq j}\varepsilon^{i,j}\left(x_i, x_j\right)}_{2-\text{way interactions}}\\ &+ 3-\text{way} + 4-\text{way}\\ &+ 5-\text{way}\cdots + d\text{-way interactions}.\end{aligned} \tag{13}$$

In this paper, the function χ is $\mathbb{E}\left[r_q\right]$, and the x_i have possible values 0 or 1 indicating presence or absence of a feature of the fluctuations on the right-hand side. The baseline ε^0 is $\mathbb{E}\left[r_q\right]$ when all features are absent (E, C, and η are set to their mean values), and main effects and interactions are evaluated by systematically adding more features (i.e., more variances and covariances) and evaluating how that changes the value of χ. An intuitive understanding of the last sentence is sufficient for reading this paper, but for completeness the rest of this paragraph explains how the terms are constructed. Let χ^A denote the response (here, the value of IGR) when features in the set $A \subseteq \{1, 2, ..., d\}$ are present and all other features are absent. The effects ε are defined at sequentially higher orders by

$$\varepsilon^A = \chi^A - \sum_{B\subset A}\varepsilon^B. \tag{14}$$

That is, ε^A is the effect of having all features in the set A present, above and beyond the sum of all main effects

of the features in A and all lower-order interactions among those features. See Hernández et al. (2023), especially sections A.4 and A.5 in Appendix S1, for more details and examples.

To reduce the number of terms and make the partition more interpretable, we did a three-feature fANOVA of Equation (12) in which the features are variation in E, in C, and in η with growth-density covariance $\mathrm{Cov}(\lambda,\nu)$ set to zero. Then, as in Johnson and Hastings (2023, eq. 28), we evaluated the contribution of growth-density covariance as the change in IGR when the $\mathrm{Cov}(\lambda,\nu)$ term is included, with all other features present.

We also carried out several sub-partitions. First: the interaction term ε^{EC} respresents the effect of variance in both E and C beyond the sum of the main effects of variance in E while C is constant, and of variance in C while E is constant. This is separated into the sum of two terms. The first term is the interactive effect of both E and C varying (with the actual marginal distributions) but with zero correlation, beyond the sum of the separate effects of having E vary while C is constant, and of having C vary while E is constant. This term is denoted $\varepsilon^{E\#C}$, the # symbol indicating that E and C have been made independent. The second term is the additional effect of covariation between E and C, denoted $\varepsilon^{\mathrm{Cov}(E,C)}$ and calculated as $\varepsilon^{EC}-\varepsilon^{E\#C}$. This separation is important because analytic MCT has identified $\varepsilon^{\mathrm{Cov}(E,C)}$ as the term measuring the contribution of the storage effect to IGR. Methods for calculating this sub-partition are described in detail by Ellner et al. (2016, 2019), and by Johnson and Hastings (2023) under small-noise assumptions that eliminate some of the terms.

Second: the $\mathrm{Cov}(E,C)$ (storage effect) and $\mathrm{Cov}(\lambda,\nu)$ (growth-density covariance) contributions were partitioned into contributions from spatial variation, from temporal variation, and from the interaction between those (conceptually very similar to the space-time decomposition of Johnson and Hastings [2023]). We define

$$E_{\mathrm{spat},q}=e^{\left(\mu_q+\sigma_{P,q}P_q(x)\right)},\qquad E_{\mathrm{temp},q}=e^{\left(\mu_q+\sigma_{W,q}W_q(t)\right)} \tag{15}$$

representing the spatial and temporal variation in the environment, respectively. We computed the spatial and temporal variance contributions to $\mathrm{Cov}(E,C)$ as $\mathrm{Cov}\left(E_{\mathrm{spat}},C\right)$ and $\mathrm{Cov}\left(E_{\mathrm{temp}},C\right)$, respectively. For $\mathrm{Cov}(\lambda,\nu)$, because E is not an isolated term, we instead repeated all the calculations to evaluate $\mathrm{Cov}(\lambda,\nu)$ with E_{spat} in place of E to get the spatial contribution, and again with E_{temp} in place of E to get the temporal contribution. Finally, the interaction term for each covariance is given by the difference between the actual value of each covariance, and the sum of the spatial and temporal contributions.

As always, the decomposition is applied to both the invading species and the resident species, and coexistence mechanisms Δ are defined as term-by-term differences between corresponding ε values for the invader and residents. If you are not familiar with why invader-resident comparisons are necessary, see the section General Theory in Ellner et al. (2019). Here we only considered two-species competition where the species have equal adult mortality and therefore equal generation times, so the invader and resident ε terms were given equal weight (Johnson & Hastings, 2022a, 2023).

METHODS: EVALUATING COEXISTENCE MECHANISMS BY SIMULATION

All model simulations were carried out using R (R Core Team, 2023) version 4.2.0 or higher for Windows, with parallelized BLAS from the Intel MKL math library (see Appendix S1: Section S6).

Generating a sample of lattice configurations with low invader population

The first step in partitioning IGR is using model simulations to find configurations of the focal species with suitably low abundance for estimating invader growth rate $\mathbb{E}\left[r_q\right]$. Because we are studying coexistence rather than invasion by a new species, we need to find configurations typical of times when the focal species has become unusually rare, starting from its typical abundance. Simulating the community and waiting for that situation to arise by chance is prohibitively time-consuming. In DS22 we used a shortcut: we started with a very small cluster and allowed its local spatial structure to equilibrate over a short time period. We presented evidence that this shortcut was a good approximation of waiting for rarity to happen by chance. But that shortcut will not work in the presence of spatial variability, because a species that has fallen from moderate abundance to rarity has just experienced a string of bad luck, and one aspect of bad luck is being concentrated in areas with below-average sites (see Appendix S1: Section S3 for details). A species growing from a small initial cluster has, instead, just experienced decent or good luck. We therefore used an

iterative method to find community trajectories leading from typical abundance to rareness of the focal species; we called our method the "limbo game" because, like the limbo dance and party game, it involves constantly lowering the bar.

For each of 50 simulated examples of the permanent spatial variability matrices $\mathbf{P}_1, \mathbf{P}_2$, we ran 300 independent simulations of the model with a 50 × 50 lattice, starting from a 50:50 mix of the two species distributed randomly in space, for 200 time steps (20 adult mean lifetimes with $\delta = 0.1$, 80 with $\delta = 0.4$). We then started the "limbo game": after each time step the simulations were paused, and the 6 replicates with the lowest abundance of the focal species (excepting those where it went extinct) were replicated 50 times each to use as the starting conditions for the next time step. This process was continued (for up to 500 time steps) until at least 25% of replicates had total abundance of the focal species equal to $G_{\max} = 25$ or less. From those final states, we chose one at random where the total abundance of the population was at least $G_{\min} = 10$ and no more than $G_{\max} = 25$.

There is nothing special about retaining 6 out of 300 parallel simulations; by trial and error, that proved effective for finding suitably small invader clusters in our model. $G_{\min} = 10$ is large enough that estimates of IGR are not biased by effects of demographic stochasticity (see DS22, Appendix S1: Section S2). $G_{\max}$ needs to be small enough that making it smaller has no meaningful effect on results; in preliminary runs we found no difference in results between $G_{\max} = 40$ and $G_{\max} = 20$ (see Appendix S1: Section S5).

The "limbo game" deliberately selects for population trajectories in which the focal species experienced especially bad environmental histories, in combination with bad luck in adult mortality and site lotteries. If there is no autocorrelation in $W_q(t)$, then atypical past environment states have no effect on future environment states. But with temporal autocorrelation, the first steps after becoming rare would strongly reflect the atypical recent history.

With continuous population density, this atypical period is transient and, therefore, can be ignored when defining invader growth rate as an (infinitely) long-term average rate. But with discrete individuals, we cannot do that: if the species is a stable member of the community, recovery from rarity may be quick rather than a long-term process. Temporal autocorrelation thus poses interesting, unresolved questions about exactly how invader growth rate should be defined for models with discrete individuals. We hope to examine this in the future, but this issue is distinct from our central questions in this paper. Here, we only consider uncorrelated temporal environmental variation.

Estimating mechanism effects through one-step-ahead averaging

Once "limbo game" simulations have generated lattices with a rare invader, the second step is using one-step-ahead model simulations to estimate the quantities needed for quantifying coexistence mechanisms. For this step, a set of $K = 50$ lattices, each representing a landscape of $\mathbf{P}_1$ and $\mathbf{P}_2$ values with mean zero and variance one was created and saved, for each of the distance scales $D = 2$, 5, and 12. These lattices were used with all values of the other parameters. The procedure is as follows: aside from limbo game it is the same as DS22, and you can see DS22 pp. 12–13 and Figure 2 for more details.

1. For each limbo game endpoint at some time T, we generated $V = 20$ independent coin-tossing simulations of adult mortality at each site. This created V vacancy configurations.
2. For each vacancy configuration, we conducted $J = 50$ independent draws of the environments $E_q(x, T)$, computed adult fertilities, dispersed larvae across sites, and simulated a random lottery at each vacant site to get the population at time $T + 1$ (note, J was denoted R in DS22, resulting in R and r having multiple meanings.)

For each of the KVJ one-step-ahead simulations (indexed by k, v and j), the actual one-step-ahead population growth rate can be expressed as in Equation (7),

$$r_q^{(j,v,k)} = \log\left[\left\langle \lambda_q\left(E_q^{(j,v,k)}(x,T), C_q^{(j,v,k)}(x,T)\right)\right\rangle + \mathrm{Cov}\left(\lambda_q^{(j,v,k)}(T), \nu_q^{(j,v,k)}(T)\right)\right] + \log\, \eta^{(j,v,k)}(T). \tag{16}$$

The E and C values were calculated from Equation (10), using $\overline{R}$ from (Appendix S1: Equation S2), λ_q values are calculated from Equation (11), and η values from Equation (6).

Equation (16) is the basis for computing the "counterfactual" population growth rates χ^{α} where features of the actual dynamics are present or absent in various combinations (see Equation (14)).

1. The estimate of the actual IGR $\mathbb{E}[r_q]$ is the average of (16) over $r_q^{(j,v,k)}$ values.
2. Variance in E was removed by setting all $E_q^{(j,v,k)}$ equal to $\mathbb{E}[E_q]$, and then re-computing $r_q^{(j,v,k)}$ values.
3. Variance in η was removed by replacing each value by its average across all KVJ one-step-ahead simulations.
4. Because of edge effects we expect the mean of C to vary by location, so variance in C was removed by

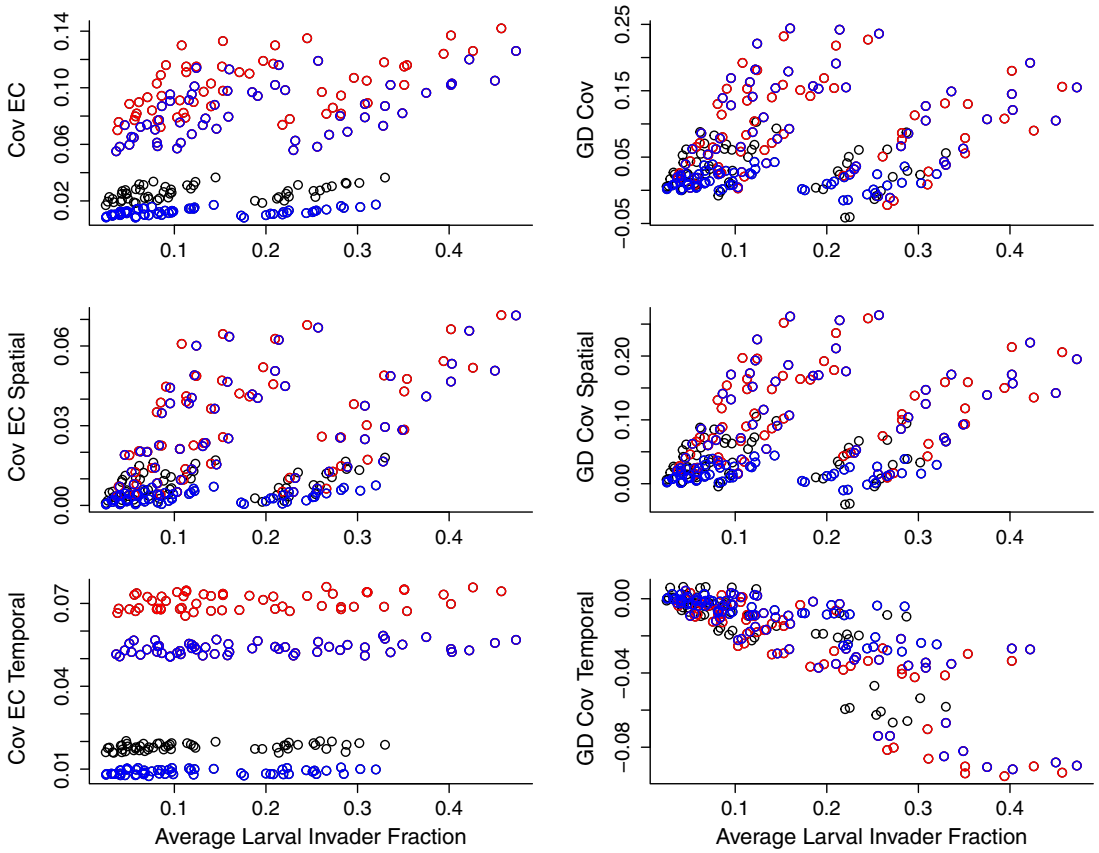

FIGURE 2 Relationship between coexistence mechanisms and average larval invader fraction. Left: Storage Effect. Right: Growth-density covariance. Top, middle, and bottom rows show the total, spatial component, and temporal component. These results are for $\sigma_P = \sigma_W = 0.25$ (black circles) or $\sigma_P = \sigma_W = 0.5$ (red circles) with $\delta = 0.2$, and $\sigma_P = \sigma_W = 0.25$ with $\delta = 0.08$ (blue circles). Figure made by R script `Graphs_HighVariance.R` available at https://doi.org/10.6084/m9.figshare.23926179.

setting the value at each location equal to its average across all *KVJ* one-step-ahead simulations. We considered several different ways to average C, but with a large M and large K, averages over lattice sites, over configurations, or over time in any combination will differ very little at nearly all sites.

5. Covariance between E and C was removed by generating new E values, from their marginal distribution but independent of C, for each of the *KVJ* replicates.
6. Spatial and temporal components of covariance terms were computed by replacing each E_q value by the corresponding spatial or temporal component (see Equation (15) and subsequent text).
7. Growth-density covariance was removed by setting $\mathrm{Cov}\left(\lambda_q^{(j,v,k)}(T), \nu_q^{(j,v,k)}(T)\right) \equiv 0$ in Equation (16).

SIMULATION STUDY DESIGN

We studied a situation where the focal species ($q = 2$) has a weak disadvantage in competition: $\mu_1 = 0, \mu_2 = -0.07$. Coexistence can, nonetheless, result from either fluctuation-independent mechanisms (a large intraspecific competition coefficient a) or fluctuation-dependent mechanisms (storage effect, growth-density covariance, relative nonlinearities in E and C). We set adult mortality $\delta = 0.2$, so that adults live 5 years on average. In DS22 we found that the value of δ affected the absolute magnitudes of coexistence mechanisms, but had no effect on any of the qualitative trends or conclusions.

Our main simulation study was a factorial design comprising all possible combinations of the following parameter values:

1. Adult intraspecific competition strength $a \in \{0.1,1\}$. The fecundity reduction from competing entirely with conspecifics rather than allospecifics is 11% when $a = 0.1$ and 50% when $a = 1$.
2. Larval dispersal parameter $\alpha \in \{0,0.12,0.4\}$, with equal values for the two species, and maximum dispersal distance always set to 15. These values produced mean dispersal distances of roughly 7.5, 5.1, and 2, respectively.

3. The spatial scale of permanent spatial variation $D \in \{2,5,12\}$.
4. Magnitudes of environmental variation $\sigma_P = \sigma_W = 0.25$ and $\sigma_P = \sigma_W = 0.5$, always with equal values for the two species. We assumed between-species correlation -0.75 for both $\mathbf{P}$ and W, so that a relatively good year or place for one is probably a relatively bad year or place for the other. As noted above, W had zero temporal autocorrelation.

Because overlapping generations is a requirement for the storage effect, we repeated the above design for $\delta = 0.08$ (mean adult lifespan of 12.5 years) restricted to $\sigma_P = \sigma_W = 0.25$. Since negative cross-species correlation in response to temporal variation favors the storage effect, we also repeated the above design with this correlation reduced to -0.35, and again with the cross-species correlation in spatial variation also reduced to -0.35, in both cases with $\sigma_P = \sigma_W = 0.5$.

RESULTS

DS22 found that the strength of the storage effect was almost entirely determined by the *average larval invader fraction*. Average larval invader fraction is defined as follows: for a randomly chosen invader larva—after larval dispersal but before the lottery for sites—what fraction of the other larvae in your site are also invaders? In DS22, for a given value of δ and σ_W, the strength of the storage effect was almost perfectly predictable from average larval invasion fraction ($R^2 > 0.9$, DS22 Figure 5). Here, with spatial variability comparable with temporal variability, we find no similarly tight link between larval invader fraction and any of the fluctuation-dependent coexistence mechanisms (Figure 2). Average larval invader fraction is still important, but it is not the only important feature.

Overall mechanism importance

The magnitudes of coexistence mechanisms are strongly dependent on the values of σ_P and σ_W, so *unless stated otherwise*, all graphs are based on results for $\sigma_P = \sigma_W = 0.5$ with $\delta = 0.2$. Additional results for $\sigma_P = \sigma_W = 0.25$ (Appendix S1: Section S7), for $\delta = 0.08$ (Appendix S1: Section S8), and for weaker cross-species negative correlation in W (Appendix S1: Section S9) or in W and $\mathbf{P}$ (Appendix S1: Section S10), all show exactly the same qualitative features.

Figure 3 summarizes the typical absolute magnitudes of the terms in the partition (left panel) and the quantiles of their distributions (right panel).

1. The baseline no-fluctuations IGR is large when $a = 1$ (strong niche differences). When $a = 0.1$ (weak niche differences) the baseline term is roughly 0 on average and never above 0.03.
2. The important fluctuation-dependent mechanisms are the covariances, as expected: EC covariance (storage effect) and growth-density covariance. Relative nonlinearity terms (in E and C) are small, and demographic stochasticity is unimportant.
3. For storage effect, the temporal component is most important; for growth-density covariance, the spatial component is most important.
4. There is sometimes a substantial interaction between the spatial and temporal components of growth-density covariance, but for storage effect there is essentially no interaction between spatial and temporal components.

Effects of dispersal scales and adult competition

Figure 4 shows how the average strengths of the main fluctuation-dependent mechanisms vary as a function of the spatial scales in the model (invader dispersal scale, resident disperser scale, and correlation scale of permanent spatial variation). To aid comparison, the same y-axis range has been used for all panels.

The storage effect contributions are remarkably constant across parameters. There is a weak negative effect of resident dispersal scale, and a weak positive effect of the scale of permanent spatial variation, which together explain over 90% of the variance in the storage effect contribution across parameters in the study. A negative effect of invader spatial scale explains an additional 2% of the variance.

The contributions of growth-density covariance have similar trends but are much more variable. The dominant trends are a positive effect of the scale of permanent spatial variation (explaining 70% of the variance) and a negative effect of resident dispersal scale (explaining 14% of the variance). The relatively small dependence on invader dispersal scale is non-monotonic, with the contribution to IGR larger at mean distance 5.1 than at mean distance 2, but slightly smaller at mean dispersal distance 7.5. When invader dispersal is highly localized (top row), the contribution of growth-density covariance is decreased (and can even be negative) with strong intraspecific competition ($a = 1$, right column, versus $a = 0.1$, left column).

These results broadly support the previously quoted conclusion of Snyder (2008) that "it is the possibility of

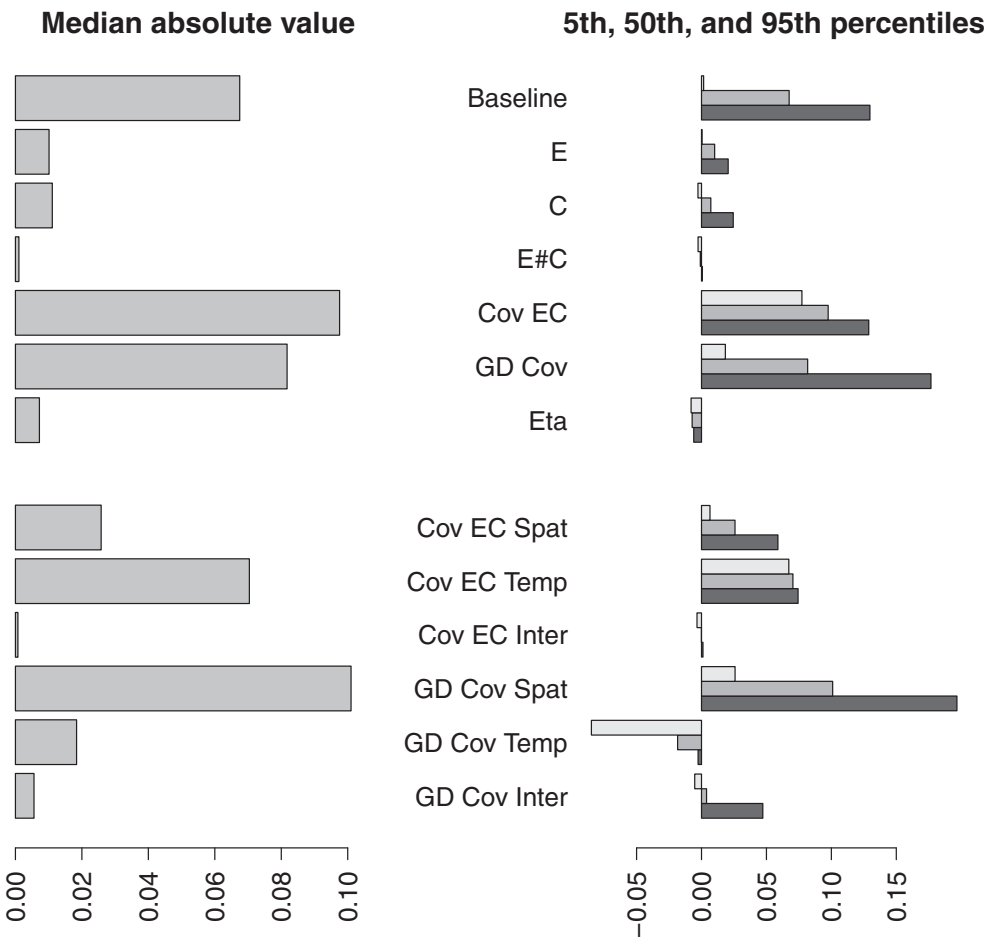

FIGURE 3 Summaries of the average absolute magnitudes of the terms in the partition (left), and quantiles of their distributions (right), for $\sigma_P = \sigma_W = 0.5$. *E#C* is the interactive effect on IGR of random variation in both *E* and *C* with their actual marginal distributions but zero correlation. "Cov *EC*" is the effect on IGR of covariance between *E* and *C*, which measures the storage effect. "Temp" and "Spat" denote the spatial and temporal components, respectively, of Cov *EC* and growth-density covariance "GD Cov," and "Inter" is the interaction of the spatial and temporal components. Figure made by R script `Graphs_HighVariance.R` available at https://doi.org/10.6084/m9.figshare.23926179.

spatial segregation which gives spatial variation its large potential to promote coexistence." We have assumed that areas good for one species are bad for another, so increases in the scale of permanent spatial variation make it easier for spatial segregation to occur through each species building up populations in distinct favorable areas. Small-scale permanent spatial variation in combination with localized invader dispersal results in the strongest impact of intraspecific competition, presumably because invaders are more tightly clustered and more likely to have conspecific neighbors.

On the other hand, it may seem counter-intuitive that growth-density covariance is affected more by resident dispersal scale than by invader dispersal scale. When IGRs are evaluated, the resident is "everywhere" while the few invaders are somewhat clustered and occupy at most 1% of sites. Why should it matter if a resident larva lands on a nearby site, which is probably occupied by a resident and surrounded by other residents, rather than a distant site which is probably also occupied by a resident and surrounded by other residents?

High growth-density covariance is the result of invaders tending to be in "good" sites: ones where their expected offspring production is high. Figure 5 shows that a crucial ingredient in that outcome is that invaders are situated where their larvae face fewer than average competitors for vacant sites. The *y* axis is proportional to the growth-density covariance term $\mathrm{Cov}(\lambda, \nu)$ in Equation (7). Points at the upper left are parameters where invaders tend to be in sites where their expected fitness is high (large *y*-axis value), and their larvae encounter relatively few other larvae (low *x*-axis value). Because most of their neighbors are residents, and invaders concentrate where conditions are good for them and bad for the resident, invaders are in locations where most of their neighbors have low fecundity. When

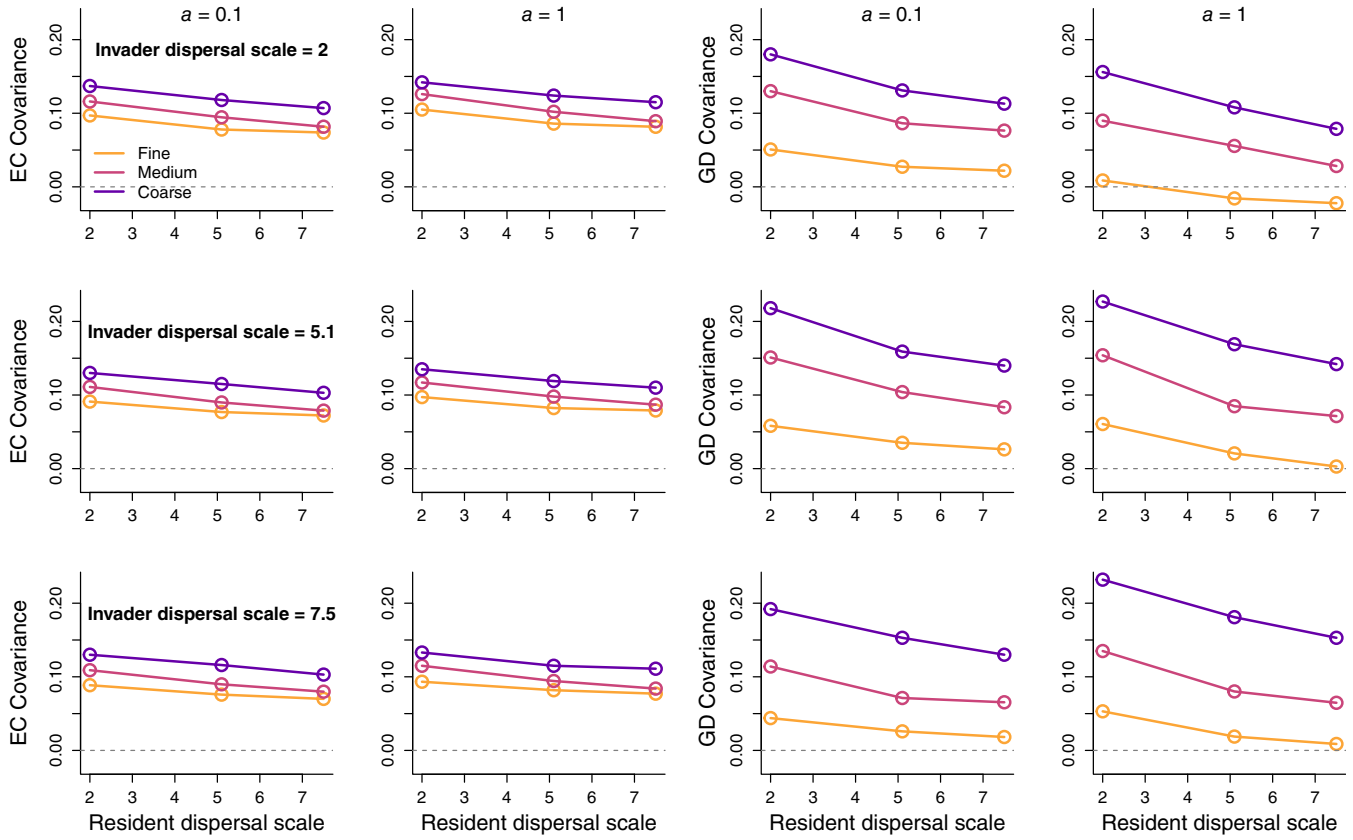

FIGURE 4 Contribution to invader growth rate (IGR) of *EC* covariance (storage effect, left half of the figure) and growth-density covariance (right half of the figure), averaged across other parameters, plotted as a function of resident species dispersal scale, for $\sigma_P = \sigma_W = 0.5$. To aid comparison, all plots use the same vertical axis scale. Colors (from light to dark) indicate the length scale of spatial patchiness (roughly 2, 5, and 12 cells). Columns differ in the value of intraspecific competition parameter a, labeled at top. Rows differ in the value of invading species dispersal scale, labeled in the leftmost column plot heading. Figure made by R script `Graphs_HighVariance.R` available at https://doi.org/10.6084/m9.figshare.23926179.

residents have short-range dispersal, many invader larvae (those not traveling too far) therefore have relatively few competitors for vacant sites, increasing invader fitness.

Long-range resident dispersal diminishes or destroys this advantage. Points at the lower right in Figure 5 reflect parameters causing invader larvae to face competition from resident larvae produced by far-away resident parents, in favorable sites, with high fecundity. Combining this with the reduced intraspecific competition in invader-rich regions, the result is that invader larvae tend to be in crowded sites, reducing invader fitness (Figure 6).

Overall, our results do not support any universal generalization about the relative strengths of storage effect and growth-density covariance. With equal SDs of variation in time and in space, either one can be the stronger. Across the parameter combinations we considered, the contribution of growth-density covariance to IGR varied much more widely than the storage effect contributions. Thus, growth-density covariance had the higher maximum strength, but for a majority (57%) of parameter combinations in our simulation study, the contribution of storage effect was larger than the contribution of growth-density covariance.

However, a comparison of spatial-versus-temporal variability mechanisms arguably should group partition terms differently. Growth-density covariance is inherently spatial, but our storage effect term includes both temporal and spatial *EC* covariance. An alternate comparison—between temporal component of storage effect, and the sum of growth-density covariance and spatial component of storage effect—is shown in Figure 6. The pattern is the same as in Figure 4, only more pronounced: the average contribution from temporal storage effect is almost constant, while the total contribution from the two spatial mechanisms varies in the same ways, but more strongly. On average, the spatial mechanisms have the wider range and higher average, and were larger than the contribution from temporal storage effect at 72% of the parameter combinations. So again, spatial mechanisms have greater potential strength, but in many situations are weaker than temporal mechanisms.

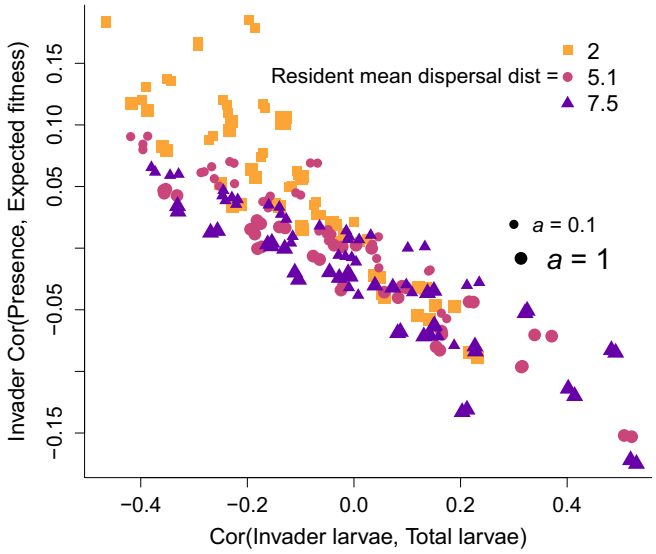

FIGURE 5 Relationship between two properties of rare invader population configurations, across different values of model parameters. The plot includes all parameter combinations described in Section *Simulation study design*. *y*-axis: Average correlation between invader presence (0 or 1 at each site) and expected invader fitness if present at that site (fitness is total number of recruits produced at all sites at the next time step). This is a measure of the degree to which invaders are found in sites where they will have high fitness (growth-density covariance). *x*-axis: Average correlation between the number of invader larvae at a site (after larval dispersal) and the total number of larvae at that site. This is a measure of how much competition a typical invader larva will face in the lottery to occupy a vacant site. The strong negative relationship shows that escape from larval competition is an important component of growth-density covariance. The two other factors having a substantial effect are the mean dispersal distance of the resident species (indicated by symbol color) and the strength of intraspecific competition (indicated by symbol size); for both, larger values have a significant negative effect (linear regression $p < 0.001$). Pairs of very close points (e.g., at bottom right) are mostly parameter sets differing only in the value of adult mortality δ. Figure made by R script `Graphs_HighVariance.R` available at https://doi.org/10.6084/m9.figshare.23926179.

DISCUSSION

Our first key finding is that the relative importance of spatial and temporal coexistence mechanisms is highly variable, as is the relative strength of the storage effect and growth-density covariance. While the strength of temporal mechanisms depended mostly on the temporal environmental variance, the strength of spatial mechanisms also varied with demographic parameters. Spatial mechanisms therefore had the greater maximum possible contribution to IGR, but also the smaller minimum contribution. This outcome was in line with our initial hypotheses. Unexpectedly, the contribution of spatial mechanisms could even be negative, opposing coexistence. Thus, intraspecific differences in habitat preferences do sometimes "overcome the negative impact of within-species clustering" (Murrell, 2010, p. 1615), but that is not always the case.

However, those conclusions have important caveats. First, like prior generalizations, they are about one model within a particular range of parameter values—a model where temporal mechanisms are especially strong (Stump & Vasseur, 2023), as we discuss below. Second, they are "all else being equal" comparisons, holding when the temporal and spatial components of environmentally-driven demographic variation have equal variance. Third, like most prior studies of similar questions they are based on two-species interactions, and results for diverse communities may be different.

Our second key finding, also unexpected, is that individual discreteness alters prior conclusions about the ecological conditions that most favor coexistence based on spatial variability. Both we and Snyder (2008) find that spatial variation promotes coexistence via spatial segregation: in particular, the invader tends to be in sites where its expected offspring production is high, as measured by the *y*-axis in Figure 5. However, the routes to segregation are different in this study, partly because of model differences but mostly because we no longer assume that competition between invader individuals is always negligible. In particular, Snyder (2008) (and earlier papers about strictly spatial variation, such as Snyder & Chesson, 2003) found that both resident and invader dispersal distances that are shorter than typical patch sizes promote coexistence, whereas we unexpectedly found that only resident dispersal distance matters very much.

This difference in results occurs because short-ranged invader dispersal is a double-edged sword in our model. Short-range dispersal still helps the invader concentrate in favorable areas, but it also exposes the invader to increased within-species competition even when it is globally rare in the community. We expected that short-range invader dispersal should still benefit invaders at least a little by enhancing spatial segregation. This expectation was borne out by growth-density covariance being largest for intermediate-range invader dispersal (Figure 4). But overly limited dispersal becomes disadvantageous: most strongly when $a = 1$, but even when $a = 0.1$. Short-range resident dispersal also benefits the invader in our model, because it promotes spatial segregation and because larvae produced by distant residents (which greatly outnumber invader larvae) do not flood invader-dominated areas.

Individual discreteness also alters the effect of intraspecific competition. Snyder (2008) found that strong,

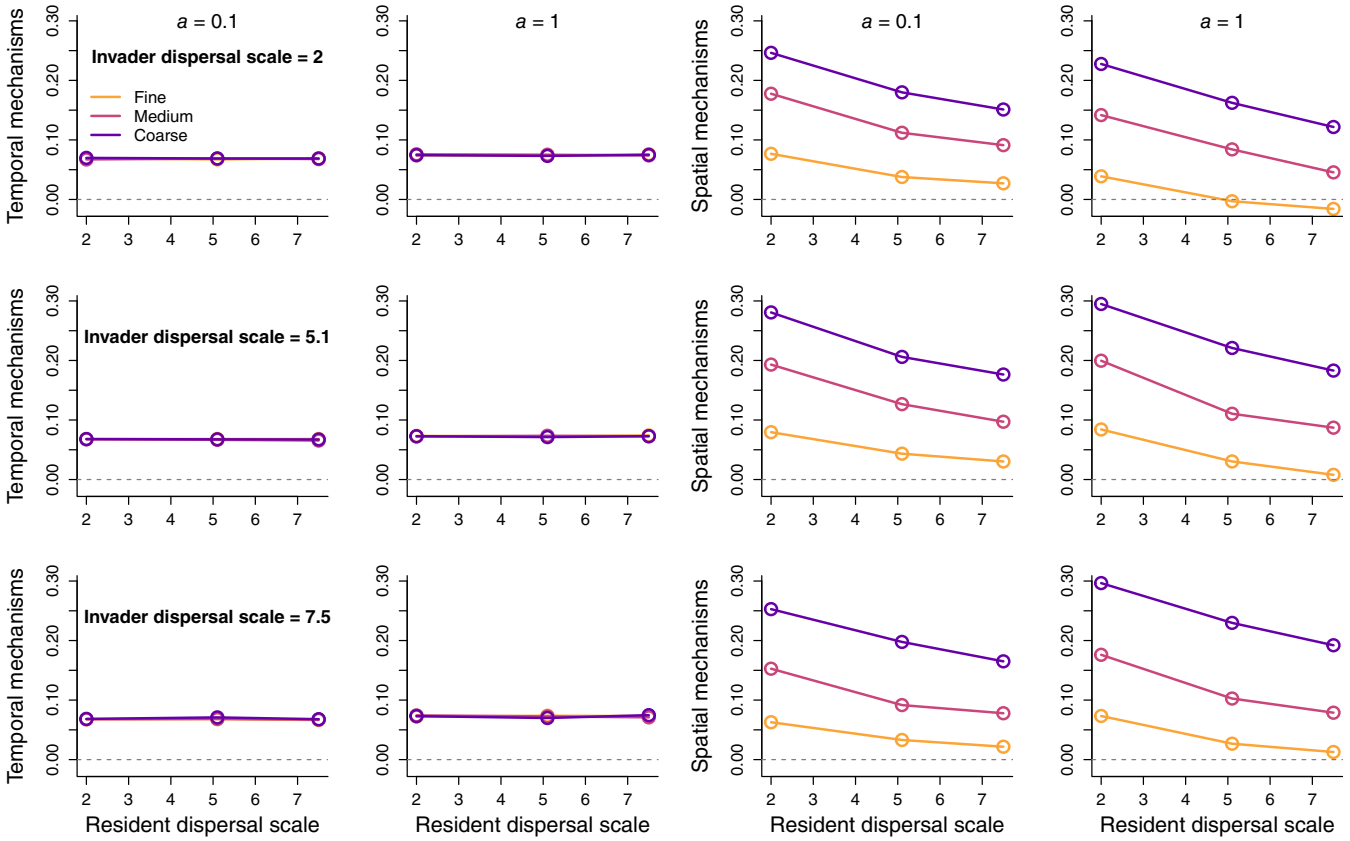

FIGURE 6 Contribution to invader growth rate (IGR) of temporal component of *EC* covariance (storage effect, left half of figure) and spatial coexistence mechanisms (growth-density covariance plus spatial component of *EC* covariance, right half of figure) averaged across other parameters, plotted as a function of resident species dispersal scale, for $\sigma_P = \sigma_W = 0.5$. To aid comparison, all plots use the same vertical axis scale. Colors (from light to dark) indicate the length scale of spatial patchiness (roughly 2, 5, and 12 cells)—note that in the left half of the figure, these curves overplot almost exactly. Columns differ in the value of intraspecific competition parameter *a*, labeled at top. Rows differ in the value of invading species dispersal scale, labeled in the leftmost column plot heading. Figure made by R script `Graphs_HighVariance.R` available at https://doi.org/10.6084/m9.figshare.23926179.

localized within-species adult competition and weak, spatially extended between-species adult competition promote coexistence. Residents then experience high competition in their favorable areas, but have little effect on distant invaders. Competition kernels in Snyder (2008) are normalized so that competition is either strong and local or weak and spatially extended. We assume that the spatial scale of competition does not vary with competition strength, so it is difficult to compare results exactly. Nonetheless, we observed that strong within-species adult competition instead *reduces* the ability of spatial segregation to promote coexistence, by contrast with Snyder (2008), again because individual discreteness allows intraspecific competition among invaders Murrell (2010).

One important direction for extending our work is to study coexistence based on regional rather than strictly local processes. In the Vellend (2010) classification of community theories, coexistence in our model is entirely due to *selection*: frequency-dependent "fitness" differences between species due to mechanisms operating at the α-diversity scale, generated by properties of the local community. At the β-diversity or metacommunity scale, where there can be substantial environmental heterogeneity among disjunct habitat patches, Mass Effect (or if you prefer, source-sink dynamics) can allow many species to coexist (e.g., Amarasekare, 2003; Hart et al., 2017; Levin, 1976; Luo et al., 2022; Myers & Harms, 2009; Shmida & Wilson, 1985). In such a setting, rare invaders concentrated in their preferred patches (or patches with conditions that an elsewhere dominant competitor cannot tolerate; Martin & Ghalambor, 2023) may still be far enough apart to avoid intraspecific competition, possibly removing the limitation that individual discreteness imposes on spatial coexistence mechanisms in our single-patch model.

Conversely, the strength of the storage effect in our model is due in part to *EC* covariance being "baked in":

if resident adults have a good year their numerous larvae face stiff competition. Features absent from the lottery model (such as between-cohort juvenile competition or rapid environmental change) can weaken the storage effect (Johnson & Hastings, 2022b; Stump & Vasseur, 2023), to the point of nonexistence: when studying coexistence mechanisms in semi-desert shrub communities, we eventually realized that we had inadvertently built models where the storage effect is structurally impossible (Ellner et al., 2016).

So unfortunately, accounting for individual discreteness only magnifies the challenge that "the devil is in the details." With a theoretician's freedom to set the rules, tilting the table to favor one outcome over another can be so easy that it happens unintentionally. The most important extension of this paper, therefore, would be to use our general methods in the context of carefully constructed empirical models for real communities. Coexistence theory is far from being complete and settled, but perhaps the greatest need now is for more Modern Coexistence Data, so that questions about coexistence mechanisms can be asked and answered about more real communities. Time-series data on population and community dynamics unavoidably accumulate slowly. To better understand coexistence, we need effective ways of combining time series with short-term observations and experiments to characterize and quantify the mechanisms that maintain community biodiversity.

AUTHOR CONTRIBUTIONS

All authors besides Christina M. Hernández contributed to conceiving and funding the project. Stephen P. Ellner and Robin E. Snyder did most of the theory and coding and wrote most of the first draft. All authors discussed all aspects of the research, and contributed to writing and revising the manuscript.

ACKNOWLEDGMENTS

This research was supported by US NSF Grants DEB-1933497 (Stephen P. Ellner, Giles Hooker, and Christina M. Hernández), DEB-1933612 (Robin E. Snyder), and DEB-1933561 (Peter B. Adler). We thank our diligent reviewers (David Vasseur, Misha Kummel, and one anonymous) who saved us from jumping to conclusions, caught many sins of omission in the original manuscript, and forced us to think more deeply about several issues.

CONFLICT OF INTEREST STATEMENT

The authors declare no conflicts of interest.

DATA AVAILABILITY STATEMENT

Code (Ellner & Snyder, 2023) is available in Figshare at https://doi.org/10.6084/m9.figshare.23926179.v3.

ORCID

Stephen P. Ellner https://orcid.org/0000-0002-8351-9734
Robin E. Snyder https://orcid.org/0000-0002-6111-0284
Peter B. Adler https://orcid.org/0000-0002-4216-4009
Christina M. Hernández https://orcid.org/0000-0002-7188-8217

REFERENCES

Amarasekare, P. 2003. "Competitive Coexistence in Spatially Structured Environments: A Synthesis." *Ecology Letters* 6: 1109–22.

Chesson, P. 1994. "Multispecies Competition in Variable Environments." *Theoretical Population Biology* 45: 227–276.

Chesson, P. 2000a. "General Theory of Competitive Coexistence in Spatially-Varying Environments." *Theoretical Population Biology* 58: 211–237.

Chesson, P. 2000b. "Mechanisms of Maintenance of Species Diversity." *Annual Review of Ecology and Systematics* 31: 343–366.

Chesson, P., and R. Warner. 1981. "Environmental Variability Promotes Coexistence in Lottery Competitive Systems." *American Naturalist* 117: 923–943.

Chesson, P. L. 1985. "Coexistence of Competitors in Spatially and Temporally Varying Environments: A Look at the Combined Effects of Different Sorts of Variability." *Theoretical Population Biology* 28: 263–287.

Ellner, S., and R. E. Snyder. 2023. "Scripts and Sample Files for the Paper 'It's About (Taking Up) Space: Discreteness of Individuals and the Strength of Spatial Coexistence Mechanisms', Initial Submission, by Ellner, Snyder, Adler, Hernandez, and Hooker." Figshare. Software. https://doi.org/10.6084/m9.figshare.23926179.v3.

Ellner, S. P., R. E. Snyder, and P. B. Adler. 2016. "How to Quantify the Temporal Storage Effect Using Simulations Instead of Math." *Ecology Letters* 19: 1333–42.

Ellner, S. P., R. E. Snyder, P. B. Adler, and G. Hooker. 2019. "An Expanded Modern Coexistence Theory for Empirical Applications." *Ecology Letters* 22: 3–18.

Ellner, S. P., R. E. Snyder, P. B. Adler, and G. Hooker. 2022. "Toward a "Modern Coexistence Theory" for the Discrete and Spatial." *Ecological Monographs* 92: e1548.

Ellner, S. P., R. E. Snyder, P. B. Adler, G. Hooker, S. J. Schreiber, and S. J. Schreiber. 2020. "Technical Comment on Pande et al. (2020): Why Invasion Analysis Is Important for Understanding Coexistence." *Ecology Letters* 23: 1721–24.

Grubb, P. 1977. "The Maintenance of Species-Richness in Plant Communities: The Importance of the Regeneration Niche." *Biological Reviews* 52: 107–145.

Hart, S., J. Usinowicz, and J. Levine. 2017. "The Spatial Scales of Species Coexistence." *Nature Ecology and Evolution* 1: 1066–73.

Hernández, C. M., S. P. Ellner, P. B. Adler, G. Hooker, and R. E. Snyder. 2023. "An Exact Version of Life Table Response Experiment Analysis, and the R Package exactLTRE." *Methods in Ecology and Evolution* 14: 939–951.

Hutchinson, G. 1961. "The Paradox of the Plankton." *The American Naturalist* 95: 137–145.

Hutson, V., and K. Schmitt. 1992. "Permanence and the Dynamics of Biological Systems." *Mathematical Biosciences* 111(1): 1–71.

Johnson, E. C., and A. Hastings. 2022a. "Methods for Calculating Coexistence Mechanisms: Beyond Scaling Factors." *Oikos* 2022: e09266.

Johnson, E. C., and A. Hastings. 2022b. "Towards a Heuristic Understanding of the Storage Effect." *Ecology Letters* 25: 2347–58.

Johnson, E. C. C., and A. Hastings. 2023. "Coexistence in Spatiotemporally Fluctuating Environments." In *Theoretical Ecology* 16: 59–92.

Levin, S. A. 1976. "Population Dynamic Models in Heterogeneous Environments." *Annual Review of Ecology and Systematics* 7: 287–310.

Luo, M., S. Wang, S. Saavedra, and F. Altermatt. 2022. "Multispecies Coexistence in Fragmented Landscapes." *Proceedings of the National Academy of Sciences of the United States of America* 119: e22015031.

Martin, P. R., and C. K. Ghalambor. 2023. "A Case for the "Competitive Exclusion – Tolerance Rule" as a General Cause of Species Turnover Along Environmental Gradients." *American Naturalist* 202: 1–17.

May, R., and R. MacArthur. 1972. "Niche Overlap as a Function of Environmental Variability." *Proceedings of the National Academy of Sciences of the United States of America* 69: 1109–13.

Murrell, D. J. 2010. "When Does Local Spatial Structure Hinder Competitive Coexistence and Reverse Competitive Hierarchies?" *Ecology* 91: 1605–16.

Myers, J., and K. Harms. 2009. "Local Immigration, Competition From Dominant Guilds, and the Ecological Assembly of High-Diversity Pine Savannas." *Ecology* 90: 2745–54.

Pande, J., T. Fung, R. Chisholm, and N. M. Shnerb. 2020. "Mean Growth Rate when Rare Is Not a Reliable Metric for Persistence of Species." *Ecology Letters* 23: 274–282.

R Core Team. 2023. *R: A Language and Environment for Statistical Computing*. Vienna: R Foundation for Statistical Computing. https://www.R-project.org/.

Shmida, A., and M. V. Wilson. 1985. "Biological Determinants of Species Diversity." *Journal of Biogeography* 12: 1–20.

Smith, H. L., and H. R. Thieme. 2011. *Dynamical Systems and Population Persistence*. Providence, Rhode Island: American Mathematical Society.

Snyder, R. E. 2008. "When Does Environmental Variation Most Influence Species Coexistence?" *Theoretical Ecology* 1: 129–139.

Snyder, R. E., and P. Chesson. 2003. "Local Dispersal Can Facilitate Coexistence in the Presence of Permanent Spatial Heterogeneity." *Ecology Letters* 6: 301–9.

Snyder, R. E., and P. Chesson. 2004. "How the Spatial Scales of Dispersal, Competition, and Environmental Heterogeneity Interact to Affect Coexistence." *The American Naturalist* 164: 633–650.

Stump, S. M., and D. A. Vasseur. 2023. "Reexamining the Storage Effect: Why Temporal Variation in Abiotic Factors Seems Unlikely to Cause Coexistence." *Ecological Monographs* 93: e1585. https://doi.org/10.1002/ecm.1585.

Vellend, M. 2010. "Conceptual Synthesis in Community Ecology." *Quarterly Review of Biology* 85: 183–206.

SUPPORTING INFORMATION

Additional supporting information can be found online in the Supporting Information section at the end of this article.

How to cite this article: Ellner, Stephen P., Robin E. Snyder, Peter B. Adler, Christina M. Hernández, and Giles Hooker. 2024. "It's about (taking Up) Space: Discreteness of Individuals and the Strength of Spatial Coexistence Mechanisms." *Ecology* e4404. https://doi.org/10.1002/ecy.4404